Effect of high donor number solvent and cathode morphology on interfacial processes in Li-air batteries

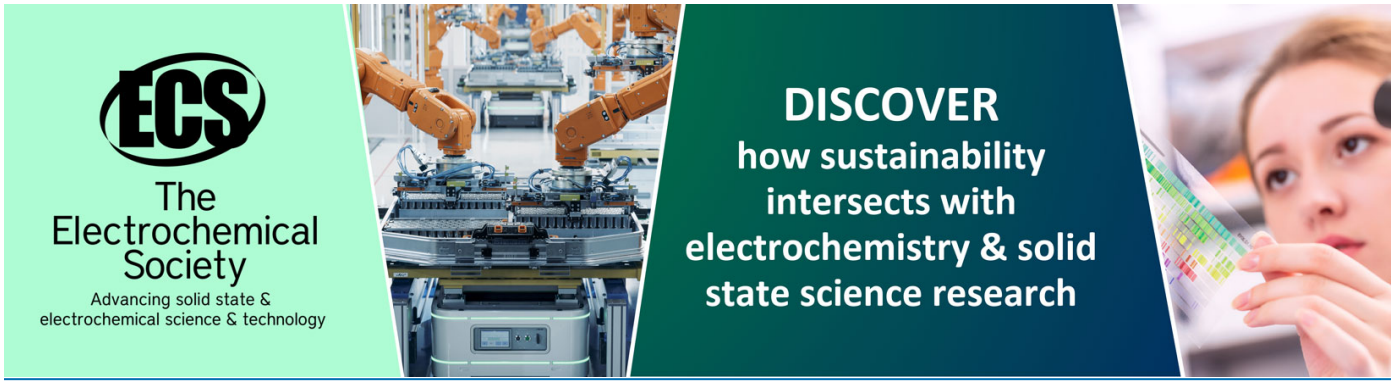

IOP Conf. Series: Journal of Physics: Conf. Series **946** (2018) 012029 doi:10.1088/1742-6596/946/1/012029

Effect of high donor number solvent and cathode morphology on interfacial processes in Li-air batteries

S A Kislenko

Joint Institute for High Temperatures of the Russian Academy of Sciences, Izhorskaya 13 Bldg 2, Moscow 125412, Russia

E-mail: kislenko@ihed.ras.ru

Abstract. The work is focused on the investigation of the effect of solvent and carbon cathode morphology on the performance of Li-air batteries. Molecular dynamics simulation was used to explore the interfacial behavior of the main reactants (O_2 and Li^+) of the oxygen reduction reaction in high donor number solvent dimethyl sulfoxide (DMSO) at the following carbon surfaces: graphene plane, graphene edge, nanotube. It was shown that the adsorption barrier of O_2 molecules decreases in the order graphene plane > nanotube > graphene edge, leading to the fastest adsorption kinetics on graphene edges. Strong solvation of Li^+ in DMSO prevents ions adsorption on defect-free graphene planes and nanotubes, which is qualitatively different from low donor number solvents, such as acetonitrile. It can be concluded from these results, that nucleation and growth of discharge products in DMSO is shifted from the surface towards the solvent bulk that, in turn, leads to capacity increase of Li-air batteries.

1. Introduction

Due to very high principally achievable energy density of cca 1 kW h/kg [1, 2], Li-air batteries are considered as an advanced alternative to Li-ion batteries. However, despite the progress in capacity improvement [3], real devices still have low electric power and cycling stability.

To solve these problems many efforts have been made to create new cathode materials based on carbon (nanotubes, fibers, graphenes etc). Effect of structural and chemical design of such materials on the oxygen reduction reaction (ORR), which takes place on a cathode surface, is the subject of thorough investigation.

It was shown that the heterogeneous electron transfer at graphene edges and open ends of carbon nanotubes is faster than at graphene plane and sidewall of nanotubes [4–9] (this effect is debated in [10]). Nitrogen- and oxygen-enriched carbon materials catalyze the ORR [11–16]. In particular, it was observed that the optimal surface oxygen atomic content of 6% on carbon nanotubes significantly improves cycling stability [16]. Porosity is another factor that should be optimized in the context of fast transport of the reactants Li^+ and O_2 and efficient deposition of discharge products (Li_2O_2, Li_2O). Increase of the mesopore volume of the cathode leads to increase in battery capacity [17–20]. Surface structure influences the mechanism of the oxygen reduction reaction [21] and morphology of discharge products [22]. It was also found that the use of cup-stacked carbon nanotubes with many edges improves the Li-air battery performance [22].

To explain such experimental results at molecular level, the ab initio DFT method is widely used. It was shown previously that catalytic effect of N-doped graphenes can be described by the decrease of the adsorption barriers and the energy difference between the Fermi level and

the unoccupied O-2p orbital level for the adsorbed oxygen molecule [23]. The carbon vacancies of graphene act as active sites due to increase in adsorption energy of O_2, LiO_2, and Li_2O_2 species [22]. CO_x groups influence the adsorption and stability of the ORR intermediates [24]. Despite the fact that these works clarify the important details of surface processes, they do not take into account the solvent effect. Meanwhile, a solvent has an ordered structure at the interface [25–30], and significantly influences the thermodynamics and kinetics of heterogeneous processes [25, 30].

In our previous work we have shown by the MD simulation that the morphology of the carbon surface affects the interface structure of acetonitrile-based electrolyte, that, in turn, influences the adsorption kinetics and concentration distribution of the reactants Li^+ and O_2 near the surface [31]. Acetonitrile is a low donor number (DN) solvent (DN = 14). At the same time, experimental investigations have shown that the type of the solvent (namely, its donor number) significantly influences the ORR mechanism, kinetics, and Li-air batteries performance [32, 33]. Since we have analyzed the low DN solvent in the work [31], it is important to estimate, how does the high DN solvent (such as DMSO) affect the behavior of the ORR reactants at the interface? We have shown previously that the interface of DMSO (DN = 30) can be restructured by the carbon surface morphology [34]. The goal of this work was to investigate the effect of such the interfacial restructuring on the thermodynamics and kinetics of Li^+ and O_2 adsorption from DMSO on different carbon surfaces (graphene plane, graphene edge, nanotube sidewall).

2. Computational details

We used the rectangular simulation box shown in figure 1. This cell contains the solvent volume of 13 nm in width confined on both sides by crystal surfaces 4.67×4.68 nm^2 in area. The right surface is the parallel-oriented three-layer graphene. The left surface is the perpendicularly-oriented multilayer graphene with armchair edges. Armchair graphene nanoribbon of 4.67 nm in width is located in the central part of the box. Single-walled carbon nanotube with the diameter of cca 0.6 nm passes through this nanoribbon in the perpendicular direction. Hydrogen atoms were attached to the edges of all graphenes for simplicity. 3D periodic boundary conditions were employed. To reduce the interaction between the simulation box and its images, the periodicity in the z direction was elongated to 25 nm.

The all-atom model compatible with CHARMM force field was used for DMSO molecules [35]. Thus, the interatomic potential parameters for C and H surface atoms were taken from the CHARMM27 force field. Carbon surface atoms were fixed during the simulation, while hydrogen atoms attached to the graphene edges were flexible. The bond stretching parameters for C–H and associated atom charges were equal to that of the benzene molecule. The parameters for O–O bond of the oxygen molecule were taken from the previous work [31]. The Lennard-Jones parameters for O and Li were taken from the CHARMM27 force field and this work [36] respectively. Charge of the Li^+ ion was scaled by a factor of $1/\sqrt{2}$ [37, 38].

The MD simulation was performed in the NVT ensemble at temperature $T = 300$ K. Nose-Hoover thermostat was used. The system contained 2229 DMSO molecules to ensure 1 bar pressure in the liquid phase. The Smoothed Particle Mesh Ewald method with a real space cutoff value of 1.5 nm was used to calculate the electrostatic interaction. The equations of motion were solved using the Verlet leapfrog integration algorithm with a time step of 1 fs. The cutoff radius of the van der Waals interaction was 1.0 nm. To generate an equilibrated system at 300 K it was first annealed at 400 during 0.2 ns. Then, the temperature was reduced to 300 K, and the systems were further equilibrated for 2 ns.

To calculate the potential of mean force (PMF) for O_2 and Li^+ the average force acting on a solute was integrated when moving it from bulk to a surface. To estimate the average force, we ran a series of MD simulations where the solute is restrained at different distances from an investigated surface with the step of 0.5 Å. In each step the force was averaged over 1 ns. To

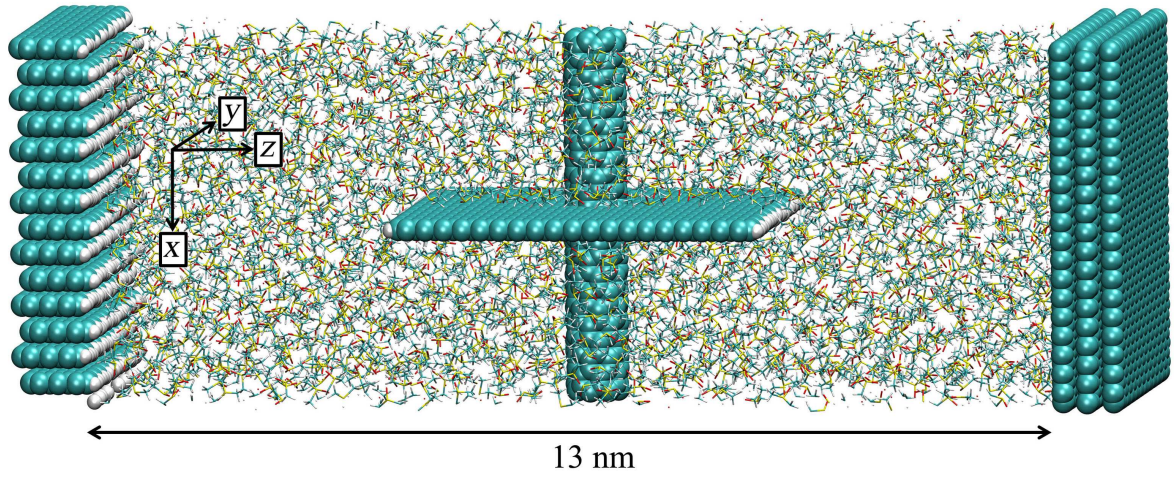

Figure 1. Snapshot of the simulation box.

calculate the PMF near the graphene edge not only the distance to the edge but the x coordinate of a solute in plane of graphene were also fixed. See paper [31] for other computational details.

We used the DL POLY classic package to perform MD simulations [39]. The calculations were run on the supercomputers MVS-100K and MVS-10P (Joint Supercomputer Center of the Russian Academy of Sciences) and "Lomonosov" (Moscow State University) [40].

3. Results and discussion

Black curve in figure 2(a) shows the potential of mean force for the O_2 molecule as a function of the distance to the graphene plane. It has an oscillating shape similar to previously published PMF in acetonitrile [31]. This effect is a result of interfacial ordering of the solvent, which has a layered structure near the surface. The correlation between the PMF and the local structure of the DMSO is observed [34, figure 3]. Minima of the solvent local density match the energy barriers that appear due to the energy consumption to move a solute from one solvent layer to another. The closest to the surface minimum of the PMF at $z = 0.35$ nm in figure 2(a) (marked as "ads.") corresponds to the adsorbed oxygen molecules; the second minimum at $z = 0.75$ nm (marked as "solv.") corresponds to the solvated ones. Thus, oxygen adsorption on the graphene plane from the DMSO solvent is an activation process this the energy barrier of cca $3k_BT$.

Figure 2(a) also shows the potentials of mean force for O_2 depending on the distance to the sidewall of the nanotube and the graphene edge (blue and red curves respectively). For ease of comparison, the potentials in the region $z < 0.75$ nm are only depicted, and zero level is set at the point $z \approx 0.75$ nm. It can be seen that the adsorption barrier decreases in the order graphene plane > nanotube > graphene edge. This can be explained by the effect, shown in our previous work [34], which consists in decreasing of the density of interfacial solvent layers with the increase of the surface curvature. Thus, the rate of oxygen adsorption (reactant feed rate) is higher on the graphene edge. This may lead to the acceleration of the oxygen reduction reaction if the adsorption rate is comparable to or slower than that of the rate-limiting step of the ORR. Qualitatively the same effect was observed in low DN acetonitrile [31]. However, the adsorption barriers in acetonitrile are smaller than in DMSO.

If the adsorption rate is significantly higher than the rate of electrochemical processes, one can calculate the equilibrium concentration distributions of reactants near the surface from the PMF using the Boltzmann equation, figure 2(b). The differences in concentration distributions

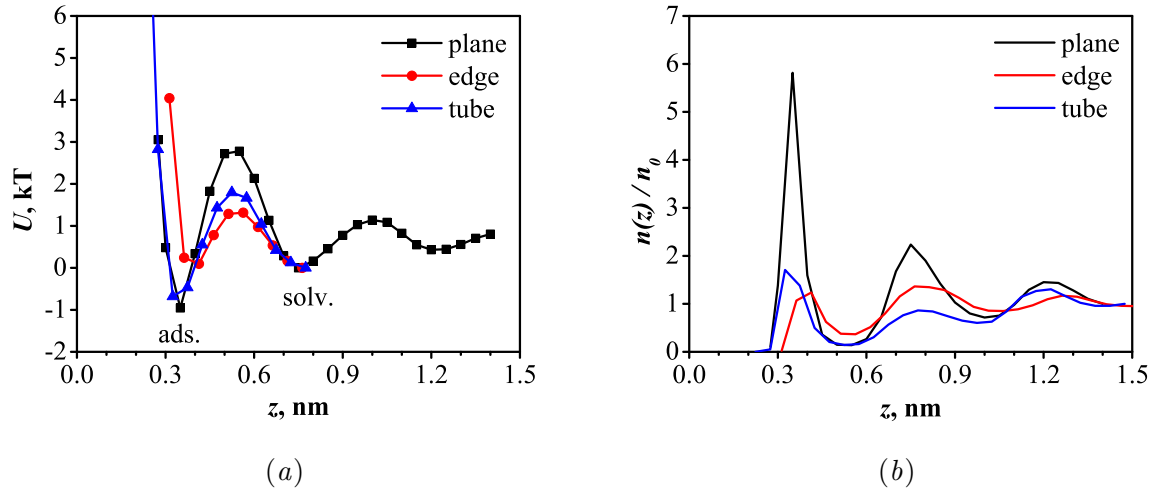

(*a*) (*b*)

Figure 2. Potentials of mean force (*a*) and concentration distributions (*b*) of O_2 ions near the graphene plane, the nanotude sidewall, and the graphene edge.

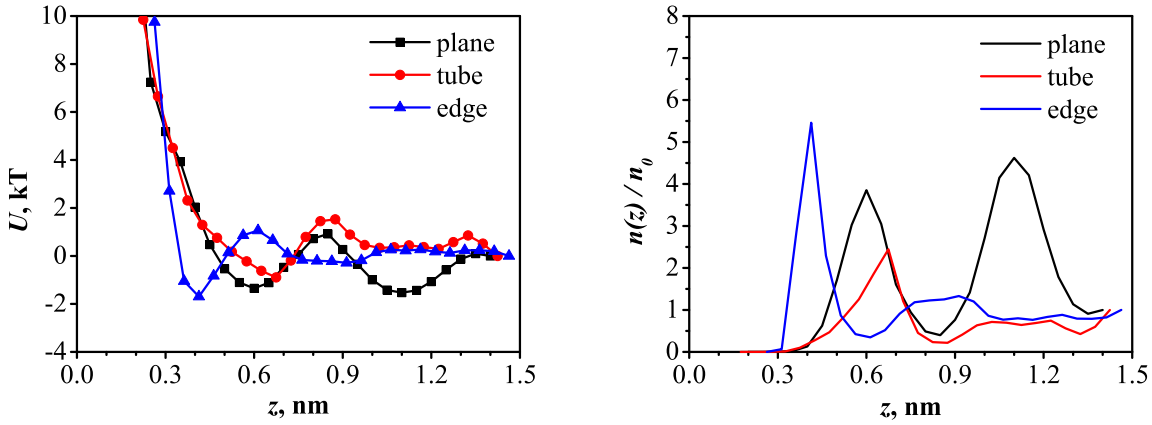

(*a*) (*b*)

Figure 3. Potentials of mean force (*a*) and concentration distributions (*b*) of Li^+ ions near the graphene plane, the nanotude sidewall, and the graphene edge.

may also explain different rate of heterogeneous electron transfer at plane and edge of the graphene [9].

Figure 3(*a*) shows the potentials of mean force for Li^+ ions as a function of the distance to the nanotube sidewall as well as to the plane and the edge of the graphene.

The potentials near the graphene plane and the nanotube are qualitatively the same. It is important to note, that in the region z = 0.3–0.4 nm, which corresponds to the position of adsorbed Li^+ ions, the local minimum are not observed. The closest to the surface minimum is at the distance cca 0.6–0.7 nm from the surface. This means that the solvent separated configuration of ions (when the ion and the surface are separated from each other by solvent monolayer) is the energetically most favorable. A qualitatively different behavior has been

observed in the low donor number solvent [31]. This effect is associated with the formation of a stable solvent shell around lithium ions in high DN solvents such as DMSO [32]. This is also in agreement with longer life-time of the superoxide O_2^- in high DN solvents due to inhibition of the association reaction with Li^+ ions [32, 33, 41]. Our simulations indicate that in DMSO (in contrast to acetonitrile) nucleation and growth of discharge products is shifted from the surface towards the solvent bulk if defect-free nanotubes and graphenes are used as an electrode material. After electron transfer to the oxygen molecule, superoxide ion O_2^- is presumably desorbed and reacts with Li^+ ions in solvent bulk. This should prevent fast passivation of the surface by insulating products (Li_2O_2, Li_2O) and result in energy capacity increase of Li-air batteries. The conclusion is in agreement with the experimental data and the qualitative model described in the work [33].

PMF for Li^+ near the graphene edge has the minimum at $z = 0.4$ nm, figure 3(a), which indicates the stability of the adsorption state of ions and results in increased concentration of Li^+ ions at the edge, figure 3(b). Coupled with fast adsorption rate, this may lead to the ORR catalysis and explain massive deposition of discharge products on graphene edges [42].

4. Conclusions

MD simulation was used to calculate the free energy profiles of the reactants O_2 and Li^+ of the oxygen reduction reaction in DMSO near different carbon surfaces: the graphene plane, the nanotube of cca 0.6 nm in diameter, and the graphene edge modified by hydrogen. The simulations show that the adsorption barrier of the O_2 molecule decreases with the increase of the surface curvature from $3k_BT$ (in case of graphene plane) to k_BT (in case of graphene edge). This gives evidence of the fastest oxygen supply at the graphene edges. The contact adsorption of Li^+ was not observed on defect-free graphenes and nanotubes (in contract to graphene edges) due to strong solvation of ions in DMSO-based electrolytes. These data are in agreement with experimentally observed increase in capacity of Li-air batteries in high DN solvents and electrocatalytic activity of graphene edges.

Acknowledgments

The present work was supported by grant from the President of the Russian Federation No. MK-7873.2016.3.

References

[1] Christensen J, Albertus P, Sanchez-Carrera R S, Lohmann T, Kozinsky B, Liedtke R, Ahmed J and Kojic A 2011 *J. Electrochem. Soc.* **159** R1–30
[2] Zheng J P, Liang R Y, Hendrickson M and Plichta E J 2008 *J. Electrochem. Soc.* **155** A432–7
[3] Xiao J *et al* 2011 *Nano Lett.* **11** 5071–8
[4] Ambrosi A, Bonanni A and Pumera M 2011 *Nanoscale* **3** 2256–60
[5] Banerjee S *et al* 2013 *ACS Nano* **7** 834–43
[6] Banks C E and Compton R G 2006 *Analyst* **131** 15–21
[7] Banks C E, Davies T J, Wildgoose G G and Compton R G 2005 *Chem. Commun.* 829–41
[8] Davies T J, Hyde M E and Compton R G 2005 *Angew. Chem.* **117** 5251–6
[9] Yuan W, Zhou Yu, Li Y, Li C, Peng H, Zhang J, Liu Z, Dai L and Shi G 2013 *Sci. Rep.* **3** 2248
[10] Patel A N, Collignon M G, O'Connell M A, Hung W O Y, McKelvey K, Macpherson J V and Unwin P R 2012 *J. Am. Chem. Soc.* **134** 20117–30
[11] Kichambare P, Kumar J, Rodrigues S and Kumar B 2011 *J. Power Sources* **196** 3310–6
[12] Kichambare P, Rodrigues S and Kumar J 2012 *ACS Appl. Mater. Interfaces* **4** 49–52
[13] Li Y, Wang J, Li X, Geng D, Banis M N, Li R and Sun X 2012 *Electrochem. Commun.* **18** 12–5
[14] Li Y, Wang J, Li X, Liu J, Geng D, Yang J, Li R and Sun X 2011 *Electrochem. Commun.* **13** 668–72
[15] Wang S *et al* 2012 *J. Mater. Chem.* **22** 21051–6
[16] Xia G, Shen S, Zhu F, Xie J, Hu Y, Zhu K and Zhang J 2015 *Electrochem. Commun.* **60** 26–9
[17] Mirzaeian M and Hall P J 2009 *Electrochim. Acta* **54** 7444–51
[18] Mirzaeian M and Hall P J 2010 *J. Power Sources* **195** 6817–24

[19] Tran C, Yang X Q and Qu D 2010 *J. Power Sources* **195** 2057–63
[20] Yang X h, He P and Xia Y y 2009 *Electrochem. Commun.* **11** 1127–30
[21] Belova A I, Kwabi D G, Yashina L V, Shao-Horn Y and Itkis D M 2017 *J. Phys. Chem.* C **121** 1569–77
[22] Nakanishi S, Mizuno F, Nobuhara K, Abe T and Iba H 2012 *Carbon* **50** 4794–803
[23] Kim H, Lee K, Woo S I and Jung Y 2011 *Phys. Chem. Chem. Phys.* **13** 17505–10
[24] Xu Y and Shelton W A 2011 *J. Electrochem. Soc.* **158** A1177–84
[25] Kislenko S A, Amirov R H and Samoylov I S 2013 *J. Phys. Chem.* C **117** 10589–96
[26] Kislenko S A, Kislenko V A and Razumov V F 2015 *Colloid J.* **77** 727–32
[27] Kislenko S A, Nikitina V A and Nazmutdinov R R 2015 *High Energy Chem.* **49** 341–6
[28] Kislenko S A, Nikitina V A and Nazmutdinov R R 2015 *Phys. Chem. Chem. Phys.* **17** 31947–55
[29] Kislenko S A, Samoylov I S and Amirov R H 2009 *Phys. Chem. Chem. Phys.* **11** 5584–90
[30] Nikitina V A, Kislenko S A, Nazmutdinov R R, Bronshtein M D and Tsirlina G A 2014 *J. Phys. Chem.* C **118** 6151–64
[31] Pavlov S V and Kislenko S A 2016 *Phys. Chem. Chem. Phys.* **18** 30830–6
[32] Abraham K M 2015 *J. Electrochem. Soc.* **162** A3021–31
[33] Johnson L, Li C, Liu Z, Chen Y, Freunberger S A, Ashok P C, Praveen B B, Dholakia K, Tarascon J M and Bruce P G 2014 *Nat. Chem.* **6** 1091–9
[34] Kislenko S A and Pavlov S V 2017 *High Energy Chem.* **51** 51–5
[35] Strader M L and Feller S E 2002 *J. Phys. Chem.* A **106** 1074–80
[36] Joung I S and Cheatham T E 2008 *J. Phys. Chem.* B **112** 9020–41
[37] Leontyev I and Stuchebrukhov A 2011 *Phys. Chem. Chem. Phys.* **13** 2613–26
[38] Leontyev I V and Stuchebrukhov A A 2009 *J. Chem. Phys.* **130** 085102
[39] Todorov I T, Smith W, Trachenko K and Dove M T 2006 *J. Mater. Chem.* **16** 1911–8
[40] Sadovnichy V, Tikhonravov A, Voevodin V and Opanasenko V 2013 "Lomonosov": Supercomputing at Moscow State University *Contemporary High Performance Computing: From Petascale toward Exascale* (Boca Raton, FL: CRC Press) pp 283–307
[41] Calvo E J and Mozhzhukhina N 2013 *Electrochem. Commun.* **31** 56–8
[42] Li Y, Wang J, Li X, Geng D, Li R and Sun X 2011 *Chem. Commun.* **47** 9438–40